

submitted to ApJ

Large Magellanic Cloud Bump Cepheids: Probing the Stellar Mass-Luminosity Relation

S. C. Keller

IGPP, L-413, LLNL, PO Box 505, Livermore, CA 94550

`skeller@igpp.ucllnl.org`

and

P. R. Wood

RSAA, Australian National University, Canberra A.C.T. 2600, Australia

`wood@mso.anu.edu.au`

ABSTRACT

We present the results of non-linear pulsation modelling of 20 bump Cepheids in the LMC. By obtaining an optimal fit to the observed V, R MACHO lightcurves we have placed tight constraints on stellar parameters of M, L, T_{eff} and well as quantities of distance modulus and reddening. We describe the mass-luminosity relation for core-He burning for intermediate mass stars. The mass-luminosity relation depends critically on the level of mixing within the stellar interior over the course of the main-sequence lifetime. Our sample is significantly more luminous than predicted by classical stellar evolutionary models that do not incorporate extension to the convective core. Under the paradigm of convective core overshoot our data implies Λ_c of $0.65 \pm 0.03 l/H_p$. We derive a LMC distance modulus of 18.55 ± 0.02 .

Subject headings: Cepheids;pulsation stellar:evolution

1. Introduction

Cepheids are classical distance indicators. Their tight conformity to a period-luminosity relationship has made them the fundamental basis of the extra-galactic distance scale and

arXiv:astro-ph/0205555v2 13 Jun 2002

hence integral to observational cosmology. Ideally, we would like to have theoretical models capable of accurately predicting the period-luminosity relation and its metallicity dependence. The regularity of Cepheid pulsation provides a set of well defined observational parameters with which to confront the predictions of theoretical models of stellar pulsations. In this way, Cepheids provide us the ability to closely scrutinise the accuracy of input physics within pulsation models.

Cepheid light curves display a variety of shapes and amplitudes that are period dependent (the Hertzsprung (1926) progression). A feature of the lightcurves of some Cepheids is a pronounced bump either preceding or following maximum. The bump arises from resonance between the fundamental mode and second overtone. This resonance becomes particularly prominent when the period ratio of these two modes ($P_0/P_2=P_{02}$) is ~ 2 .

The bump enables us to break the degeneracy that exists between observable quantities; lightcurve shape, amplitude, period and the intrinsic properties; mass, luminosity and temperature of the Cepheid. Such a technique was first proposed by Stobie (1969) and was demonstrated by Wood, Arnold, & Sebo (1997)(hereafter Paper 1) in their non-linear pulsation analysis of the LMC bump Cepheid HV 905.

Through the analysis of bump Cepheids we have a probe of the stellar mass-luminosity (M-L) relation for core He-burning stars. The M-L relation depends critically on the size of the central He core established (largely) during the course of the star’s main-sequence lifetime. The size of the He core is in turn, determined by the extent of convection in the vicinity of the convective core.

The treatment of convection remains the weakest point in our description of massive stars. Ongoing debate focuses on the degree of extension to the convective core beyond that predicted by standard, non-rotating stellar evolution models. Extension of the convective core has traditionally been discussed in terms of convective core overshoot (CCO) in the formalism of mixing-length theory. The CCO parameter, Λ_c , sets the height (as a fraction of the pressure scale height) to which gas packets from the convective core rise into the formally convectively stable region surrounding the core.

Mixing in the vicinity of the convective core produces a number of important evolutionary changes that are expressed in a stellar population. It expands the amount of H available to the core and hence extends the main-sequence lifetime. The star consequently develops a more massive He core and the subsequent post-main-sequence evolution occurs at a more rapid pace and at higher luminosities. That is, the M-L relation is significantly more luminous than that of classical models.

Numerous studies have attempted to ascertain the efficiency of CCO from a theoret-

ical basis with results that range from negligible to substantial (see e.g. Bressan, Chiosi, & Bertelli (1981)). An analytical approach appears limited given the complexity of the phenomenon. Laboratory fluid dynamics shows that an understanding of convective mixing requires a description of the turbulence field at all scales, a problem that will require detailed hydrodynamical modelling.

Observations are required to ascertain the amount of CCO to apply in stellar evolutionary models. Many studies have sought to do so through the study of young cluster populations (most recently Barmina et al. (2002); Keller, Da Costa, & Bessell (2001)) and from the broader field population (Beaulieu et al. 2001; Cordier et al. 2002) of the Magellanic Clouds. Whilst large uncertainties exist in the derived values of Λ_c , the broad consensus of these studies is the necessity of some level of CCO.

Another way of quantifying Λ_c is to use masses and luminosities of Cepheids. Dynamical masses for Cepheids are presented by Evans et al. (1997, 1998) and Bohm-Vitense et al. (1997a,b). Derived masses have considerable uncertainties but the combined sample (Evans et al. 1998) indicates the necessity for some level of CCO.

This study aims to quantitatively establish the level of CCO by an examination of the M-L relation of a sample of bump Cepheids from the LMC. A consistent result of pulsation modelling is that the M-L relation for Cepheids is significantly brighter than predicted by classical stellar evolution. The study of the bump Cepheid HV905 in Paper 1 found a bump mass 29% lower than that required by evolutionary models without CCO. Recently, Bono, Castellani, & Marconi (2002) applied non-linear modelling techniques that incorporate turbulent convection to two LMC bump Cepheids. They found that an acceptable match between model and observed lightcurves required a mass-luminosity relation in which stars are $\sim 15\%$ lower in mass than predicted by evolutionary models that neglect convective core overshoot. Linear pulsation analyses (Sebo & Wood 1995; Kanbur & Simon 1994) similarly require pulsation masses for Cepheids that are significantly lower than evolution masses.

2. Observations

Photometry for the LMC bump Cepheids considered here is taken from the MACHO photometric database. Stars are only considered from the central bar region (the top 22 MACHO fields) in which standardised photometry exists. Magnitudes in the MACHO B and R passbands have been converted to Kron-Cousins V and R using existing transformations described in Alcock et al. (1999). Photometric uncertainties are quoted as ± 0.035 mag in zero point and $V-R$ colour. The observed Cepheids are listed in Table 1.

3. Model Details

Details of the non-linear pulsation code are given in Paper 1. The opacities have been updated to OPAL 96 (Iglesias & Rogers 1996), supplemented at low temperatures by those of Alexander & Ferguson (1994). Convective energy transport was included by means of mixing-length theory with the assumption of a mixing length of 1.6 pressure scale heights. A linear non-adiabatic code was used to derive the starting model for each simulation. Models contained 460 mass points outside an inner radius of $0.3 R_{\odot}$. Transformation of L and T_{eff} into V and $V-R$ of our observations was made through interpolation into a grid of synthetically derived colours and bolometric corrections. The colors were computed for the revised Kurucz (1993) fluxes used in Bessell, Castelli, & Plez (1998) and described in more detail in Castelli (1999). Magnitudes were computed through energy integration using the passbands of Bessell (1990). We computed non-linear models at a fixed composition of $Y=0.27$ and $Z=0.008$ found for young objects in the LMC (Russell & Bessell 1989).

In contrast to Bono, Castellani, & Marconi (2002), our method uses only stellar pulsation and stellar atmosphere theory, we do not make recourse to existing mass-luminosity (M-L) relations. Once abundance is assumed three parameters, M , L and T_{eff} remain to characterise the pulsating envelope of each Cepheid. Thus three conditions are required to determine these quantities.

The first condition is that the fundamental pulsation period of the starting linear models must satisfy the observed period of the Cepheid. The other two conditions come from fitting non-linear model lightcurves to the observations. The two parameters we chose as independent variables for the lightcurve fit were T_{eff} and P_{02} , the ratio of the fundamental to second overtone periods. The amplitude of pulsation is dependent on the star’s temperature relative to the blue edge of the IS. Hence the amplitude of pulsation is a strong constraint on T_{eff} . The phase of the bump is dependent on P_{02} and furthermore, is independent of the pulsation amplitude (Simon & Lee 1981).

To commence the modelling process values of T_{eff} and P_{02} were specified and parameters L and M were iterated until the required linear period and P_{02} were produced. Once model parameters were determined, the static model was perturbed with the eigenfunction of the linear adiabatic fundamental mode. The perturbed model was run until the kinetic energy of the pulsation reached a limit cycle.

Our models incorporate convective energy transfer through the mixing length approximation. This is known to be only a partial description of the internal physics in a Cepheid atmosphere. In particular, at cooler temperatures as the convective regions become larger and the dynamical timescale becomes a significant fraction of the pulsation period our models

are expected to become increasingly divergent. This is a well known shortcoming of models that implement the mixing-length approximation. Whilst our models can match the blue edge of the instability strip (IS) they can not reproduce its red edge. In the vicinity of the red edge the amplitude of pulsation is too high, a feature that can not be circumvented by modification of artificial viscosity parameters. To produce a physical red edge an additional form of energy dissipation is required. Convective processes are the likely cause of this. Yecko, Kollath, & Buchler (1998) shows that models with a parametrised formulation of turbulent convective mixing are able to match the fundamental and first overtone instability strips through a fine tuning of parameters.

Yecko et al. consider the case of a $5M_{\odot}$ star modeled both with mixing-length approximation and with turbulent convection. Consideration of the model growth rates (their figure 11) shows insignificant differences over the bluest 1/4 of the IS, becoming increasingly divergent thereafter. In order to avoid as much as possible the short comings of the mixing-length approach we have sought bump Cepheids close to the blue edge of the IS (see Fig. 1).

4. Results

In figures 2 & 3 we show the effects of variation of the two parameters T_{eff} and P_{02} . As we change P_{02} we modify the phase at which the bump is located. Similarly, as T_{eff} is varied the amplitude is changed. The best fit to the observed light curve is shown in the central panel. Here for the purpose of illustration we show five models widely separated in parameter space. In the determination of the best model, however, we use a iterative chi-squared minimisation technique.

The offset of the model M_V and observed V light curves gives the apparent distance modulus. Having obtained a model that matches the V light curve of each bump Cepheid, the observed $V-R$ colour curve was shifted onto the model intrinsic $V-R$ colour curve. The shift required to do so is the colour excess, E_{V-R} , which can be converted to visual absorption, A_V , using a standard reddening curve ($A_V=1.78E(V-R)$ was used). The true distance modulus can then be obtained from the apparent distance modulus. The best fit parameters for the Cepheids in our sample are given in Table 2.

Limits of *internal* accuracy in the determination of the best model solution arises from cycle-to-cycle variations in the model output. By monitoring on the order of 30 cycles we can quantify the uncertainty introduced by these model variations. The errors in the determined parameters are dominated by the uncertainty in P_{02} . This becomes problematic towards lower masses as the bump amplitude diminishes. *Systematic* uncertainties dominate the total

uncertainty however. The quoted photometric uncertainties for the MACHO photometry account for $\pm 0.1M_{\odot}$ in mass and ± 0.002 dex in luminosity. Error bars shown in figure 4 are the quadrature sum of systematic and internal uncertainties.

As stated above, a value of metallicity is adopted in our analysis. It is important to remark on the effects that varying this metallicity has on our models. An exploration of this has been presented by us in Paper 1. In this work, models were additionally constructed for solar and SMC metallicities. It was found that the models cannot be used to distinguish the abundance of the Cepheid with any meaningful uncertainty. If the abundance of our sample is assumed to lie in the range $Z=0.006-0.01$ and $Y=0.25-0.29$ the resulting error in the derived parameters from the uncertainty due to abundance is of similar magnitude as that reported from P_{02} and T_{eff} .

A less constrainable systematic effect may arise from our treatment of convection. We note the work of Buchler et al. (1996) and Feuchtinger, Buchler & Kollath (2000) who find that the effects of convection are important even in the vicinity of the blue edge. Whilst a large degree of freedom is available in the internal parameters of turbulent convection models the magnitude of this possible systematic effect remains uncertain.

4.1. Reddenings and Distance Modulus

Another independent prediction of the bump Cepheid models is the reddening to each object. In figure 5 we present the histogram of determined reddenings. Our derived mean reddening is 0.08.

A number of studies of line-of-sight reddening to LMC stars have been presented in the literature. Bessell (1991) showed that the historically low values for reddening to the LMC ($\langle E(B-V) \rangle \sim 0.03$) were too low and used the Johnson & Morgan reddening-free Q index and spectroscopic temperatures to show that the $\langle E(B-V) \rangle \sim 0.12$. Harris, Zaritsky, & Thompson (1997) use Q to form a histogram of $E(B-V)$ from a $2.8^{\circ 2}$ region of the LMC. They find a mean reddening of 0.20 with a non-gaussian tail extending to higher $E(B-V)$. Larsen, Clausen, & Storm (2000) report $\langle E(B-V) \rangle = 0.085$. Zaritsky (1999) revisits the data of Harris et al. and reports a strong dependence of $\langle E(B-V) \rangle$ on the spectral type of objects used to define it. Namely, low extinctions result from red clump stars, high extinction from OB stars. Zaritsky proposes that is the result of a larger scale height for older stars, placing them statistically in lower reddening regions than the OB stars that reside in the dusty disk. With this background we find that our reddenings are applicable for objects within the LMC.

The mean LMC distance modulus shown in Figure 5 is 18.55 ± 0.02 . This in good agreement with recent analysis (18.57 ± 0.14 from the compilation of Gibson 2000).

The consistency of our derived reddening and distance modulus with previous studies provides a validation to the input of our model. It means that the results we present here will be consistent with results derived from linear pulsation models. Linear pulsation models that utilize the observed colours, reddenings, apparent luminosity and distance modulus by Sebo & Wood (1995) do indeed show pulsation masses for LMC Cepheids that are similarly lower than evolution masses. This gives us confidence in the consistency of the linear and non-linear pulsation theory as well as the bolometric corrections and colour transformations.

4.2. The Mass-Luminosity Relation

By modelling the bump Cepheid sample we have independently determined both L and M for each object. We use these values to construct the mass-luminosity relation for core-He burning stars in the LMC. Figure 4 shows the mass-luminosity relationship described by our sample. Overlaid are the M-L relations (due to Fagotto et al. (1994) and Bressan (2001)) for three levels of convective core overshoot efficiency with $Z=0.008$ and $Y=0.25$.

The data are significantly more luminous than the predictions of standard “mild” convective core overshoot (i.e. $\Lambda_c = 0.5$). Figure 4 recommends a degree of convective core overshoot of $\Lambda_c = 0.65 \pm 0.03l/H_p$. Put another way, our results favour a mass $19.5 \pm 1.0\%$ lower than classical evolutionary models.

The problem of reconciling mass determinations from the various techniques available has been a problem that has plagued the field. The many phases of debate, and their convergence, have been extensively discussed in the literature (see e.g. Cox (1980)). The longest standing of these, the bump and beat Cepheid mass discrepancy, has to a large part been resolved by Moskalik, Buchler, & Marom (1992) through the introduction of OPAL opacities. The discrepancy between pulsation and evolutionary mass has not been removed by improvements in input physics.

One possibility that has been suggested by Bono, Castellani, & Marconi (2002) is that mass loss is responsible for the reduction in mass. As opposed to the evolutionary models used in the study of Bono et al. that neglect mass loss, the models shown in figure 4 incorporate the mass loss prescription of de Jager et al. (1988). This is largely responsible for the curvature of the M-L relation towards higher masses. Furthermore, mass loss during the Cepheid phase does not appear to be enhanced from that expected from the de Jager description (Deasy 1988). We conclude that mass loss alone can not explain the Cepheid mass discrepancy.

One Cepheid (MACHO 2.4661.3597: HV 905) has been the target of previous analysis in Paper 1. However, the current work uses updated OPAL opacities and improved low temperature opacities from Alexander & Ferguson (1994), and replaces bolometric corrections of Kurucz (1993) with those of Castelli (1999). The results from this previous work were $M=5.15\pm 0.35M_{\odot}$ and $\log(L/L_{\odot})=3.69\pm 0.01$ (uncertainties determined post-fact from the details presented in Paper 1). Here we find $M=5.62\pm 0.22M_{\odot}$ and $\log(L/L_{\odot})=3.701\pm 0.004$.

In their description of their non-linear pulsation models that incorporate turbulent convection, Bono, Marconi, & Stellingwerf (1999) compare their model output for HV 905 with that of Paper 1. They use the mass, luminosity, T_{eff} and abundance in Paper 1 and retrieve a limit cycle lightcurve that is very similar in shape to that of Paper 1. In addition, the P_{02} differs by only 1% and the luminosity amplitude differs by 0.06-0.08 mag from that presented in Paper 1. This gives us confidence that our study is unaffected by our treatment of convection under the mixing length approximation.

Future refinement of the technique described here is possible through the comparison of observed radial velocity variations of bump Cepheids to those predicted by our model. This has the benefit of limiting systematic errors. At present, the accuracy of our technique is limited by systematic photometric uncertainties (in particular transformations of MACHO bandpasses and zeropoints). The radial velocity curve is a more robust output of the non-linear pulsation model. Radial velocities are more closely related to the dynamical processes within the stellar atmosphere than that of photometry which is more affected by temperature changes than dynamical effects. Work is currently underway by us to use radial velocity curves for bump Cepheids as a stringent test on our pulsation models. Models should be able to accurately reproduce all observational constraints (period, shapes of light *and* velocity curves). Such a critical examination of the dynamics of Cepheid pulsation offers the potential of further model refinement.

We note that demonstrating the convective core is of greater extent than the core defined by the Schwarzschild criterion does not determine its causation. Recent studies have shown that rotation can provide a natural way to bring about increased internal mixing and hence a larger core (Heger, Langer, & Woosley 2000; Meynet & Maeder 2000).

Attention to rotational mixing has been promoted by the findings of chemical abundance studies of A supergiants (Venn 1995), B supergiants (Dufton et al. 2000), and main-sequence B stars (Daflon et al. 2001; Gies & Lambert 1992) which imply a broad range of enhancements. This behavior is interpreted as arising from self-contamination with CN-cycled material prior to the first dredge-up. Such surface modifications can not be achieved through CCO.

Furthermore, the CNO abundances for a set of 10 SMC A supergiants have been studied by Venn (1999). These stars show a large range in N abundance enhancements ranging from negligible to levels greater than first dredge-up. The magnitude of enhancement is much greater than that found for a similar sample of Galactic A supergiants (Venn 1995) which suggests a possible metallicity effect in the underlying physics of internal mixing.

Bump Cepheids of the SMC offer the opportunity to investigate the metallicity dependence of internal mixing. A greater level of internal mixing such as would be produced by generally higher stellar rotation velocities in the SMC (Venn 1999) should result in a clear modification of the M-L relation. Work is underway to look for such effects.

5. Conclusions

In this study we have applied non-linear pulsation models to match the observed light and colour curves of 20 LMC bump Cepheids. We have been able to place tight constraints on the stellar parameters mass, luminosity and effective temperature as well as individual reddenings. We have described the mass-luminosity relation over the mass range of bump Cepheids. We find our sample is $\sim 20\%$ more luminous for their mass predicted by stellar evolution models that do not incorporate extension to the convective core. Under the paradigm of convective core overshoot this amounts to Λ_c of $0.65 \pm 0.03 l/H_p$. The models yield an LMC distance modulus of 18.55 ± 0.02 .

We thank A. Bressan et al. for providing us with unpublished evolutionary models for $\Lambda_c=1.0$. We thank our referee Dr. Z. Kollath for his comments and personal calculations regarding systematic effects due to turbulent convection. Work performed by SCK was performed under the auspices of the U.S. Department of Energy, National Nuclear Security Administration by the University of California, Lawrence Livermore National Laboratory under contract No. W-7405-Eng-47.

REFERENCES

- Alexander, D. R. & Ferguson, J. W. 1994, *ApJ*, 437, 879
- Alcock, C. et al. 1999, *PASP*, 111, 1539
- Barmina, R., Girardi, L., Chiosi, C. 2002, *A&A* accepted, astro-ph/0202128
- Beaulieu, J.P., Buchler, J.R. & Kollath, Z. 2001, *A&A*, 373, 164

- Bessell, M. S. 1990, *PASP*, 102, 1181
- Bessell, M. S. 1991, *A&A*, 242, L17
- Bessell, M. S., Castelli, F., & Plez, B. 1998, *A&A*, 333, 231
- Böhm-Vitense, E., Evans, N. R., Carpenter, K., Morgan, S., Beck-Winchatz, B., & Robinson, R. 1997b, *AJ*, 114, 1176.
- Böhm-Vitense, E., Remage Evans, N., Carpenter, K., Beck-Winchatz, B., & Robinson, R. 1997a, *ApJ*, 477, 916.
- Bono, G., Castellani, V., & Marconi, M. 2002, *ApJ*, 565, L83
- Bono, G., Marconi, M., & Stellingwerf, R. F. 1999, *ApJS*, 122, 167
- Bressan, A. G., Chiosi, C., & Bertelli, G. 1981, *A&A*, 102, 25
- Bressan, A. G., 2001, priv. comm.
- Buchler, J. R., Kollath, Z., Beaulieu, J.-P. & Goupil, M. J., *ApJ*, 462, L83
- Castelli, F. 1999, *A&A* 346, 564
- Chiosi, C., Wood, P.R., & Capitanio, N. 1993, *A&AS*, 86, 541
- Cordier, D., Lebreton, Y., Goupil, M.-J., Lejeune, T., Beaulieu, J.-P. & Arenou, F. 2002, *A&A* submitted
- Cox, A. N. 1980, *ARA&A*, 18, 15
- Dafon, S., Cunha, K., Butler, K., & Smith, V. V. 2001, *ApJ*, 563, 325
- de Jager, C., Nieuwenhuijzen, H., & van der Hucht, K. A. 1988, *A&AS*, 72, 259
- Deasy, H. P. 1988, *MNRAS*, 231,
- Dufton, P. L., McErlean, N. D., Lennon, D. J., & Ryans, R. S. I. 2000, *A&A*, 353, 311
- Evans, N. R., Böhm-Vitense, E., Carpenter, K., Beck-Winchatz, B., & Robinson, R. 1998, *ApJ*, 494, 768
- Evans, N. R., Böhm-Vitense, E., Carpenter, K., Beck-Winchatz, B., & Robinson, R. 1997, *PASP*, 109, 789
- Fagotto, F., Bressan, A., Bertelli, G., & Chiosi, C. 1994, *A&AS*, 105, 29

- Feuchtinger, M., Buchler, J. R. & Kollath, Z. 2000, ApJ, 544, 1056
- Freedman, W. L. et al. 2001, ApJ, 553, 47
- Gibson, B. 2000, Mem. Ast. It., astro-ph/9910574
- Gies, D. R. & Lambert, D. L. 1992, ApJ, 387, 673
- Harris, J., Zaritsky, D., & Thompson, I. 1997, AJ, 114, 1933
- Heger, A., Langer, N., & Woosley, S. E. 2000, ApJ, 528, 368
- Hertzsprung, E. 1926, Bull. astronom. Inst. Netherl., 3, 115
- Iglesias, C.A. & Rogers, F.J. 2996, ApJ, 464, 943
- Kanbur, S. M. & Simon, N. R. 1994, ApJ, 420, 880
- Keller, S. C., Da Costa, G. S., & Bessell, M. S. 2001, AJ, 121, 905
- Kurucz, R.L. 1993, CD-ROM No. 13. Cambridge, Mass.: Smithsonian Astrophysical Observatory
- Larsen, S. S., Clausen, J. V., & Storm, J. 2000, A&A, 364, 455
- Meynet, G. & Maeder, A. 2000, A&A, 361, 101
- Moskalik, P., Buchler, J. R., & Marom, A. 1992, ApJ, 385, 685
- Russell, S. C. & Bessell, M. S. 1989, ApJS, 70, 865
- Sebo, K. M. & Wood, P. R. 1995, ApJ, 449, 164
- Simon, N. R. & Lee, A. S. 1981, ApJ, 248, 291
- Stobie, R. S. 1969, MNRAS, 144, 511.
- Stothers, R. B. & Chin, C. 1992, ApJ, 390, 136
- Venn, K. A. 1999, ApJ, 518, 405
- Venn, K. A. 1995, ApJ, 449, 839
- Wood, P. R., Arnold, A., & Sebo, K. M. 1997, ApJ, 485, L25 (Paper 1)
- Yecko, P. A., Kollath, Z., & Buchler, J. R. 1998, A&A, 336, 553

Zaritsky, D. 1999, AJ, 118, 2824

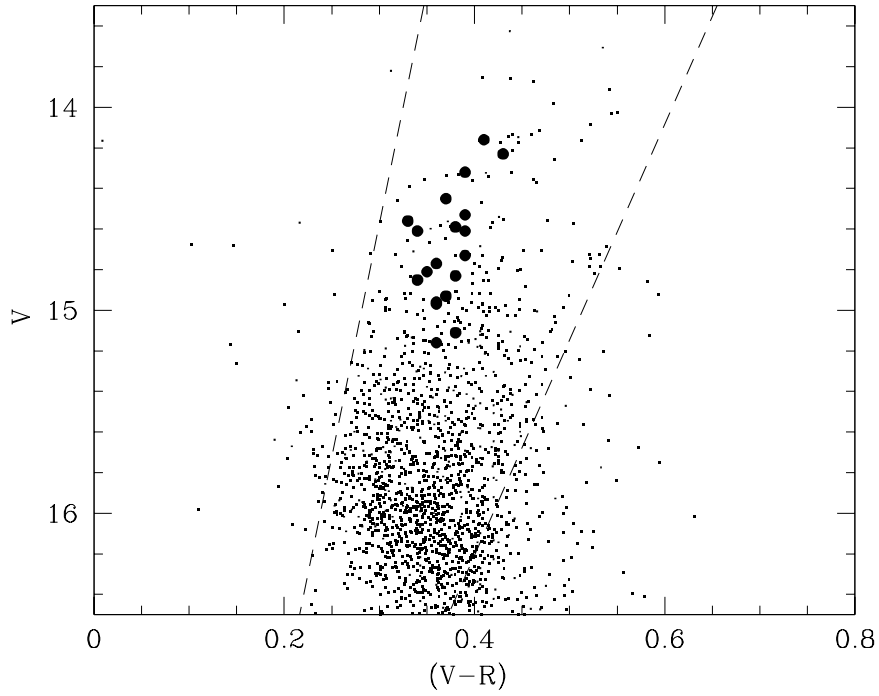


Fig. 1.— The V , $V-R$ colour-magnitude diagram for fundamental Cepheids in the MACHO catalogue. The bump Cepheids of the present study are shown in bold. Overlaid are the blue and red edge of the instability strip described by Chiosi, Wood & Capitano (1993) assuming $E(B-V)=0.12$

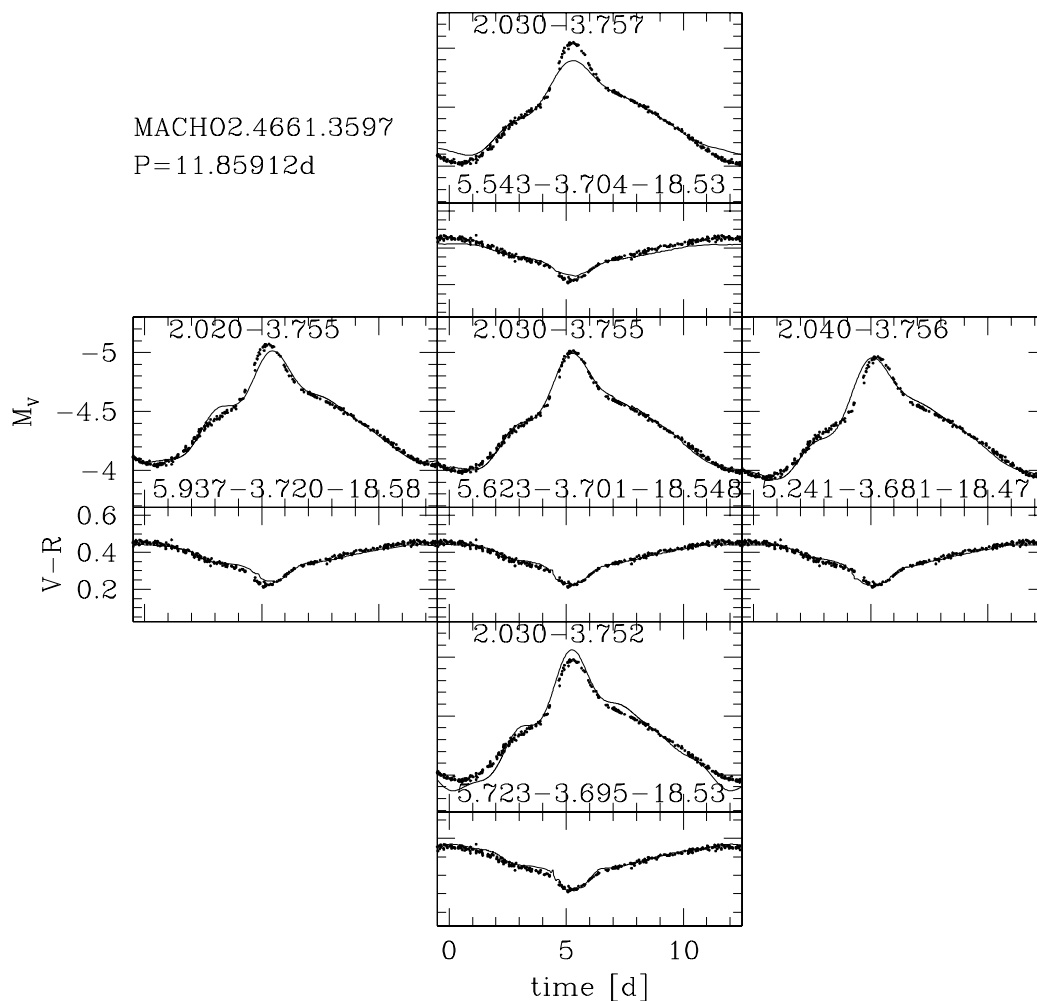


Fig. 2.— Model fits for MACHO 2.4661.3597. The numbers in each panel are: the period ratio P_{02} and $\log T_{eff}$ in the upper part, and M/M_{\odot} , $\log L/L_{\odot}$, and the true distance modulus in the lower part. Each panel contains light and color curves (dereddened). Observations are shown as dots and models as lines. The panels in the vertical section show the effect of changing T_{eff} , this affects the amplitude (in the upper panel T_{eff} is too large, the resulting amplitude is too low). The horizontal section shows the effect of a changing P_{02} this affects the phase of the bump (in the left panel P_{02} is too small, the phase of the bump is too “late”). The central panel is the best model.

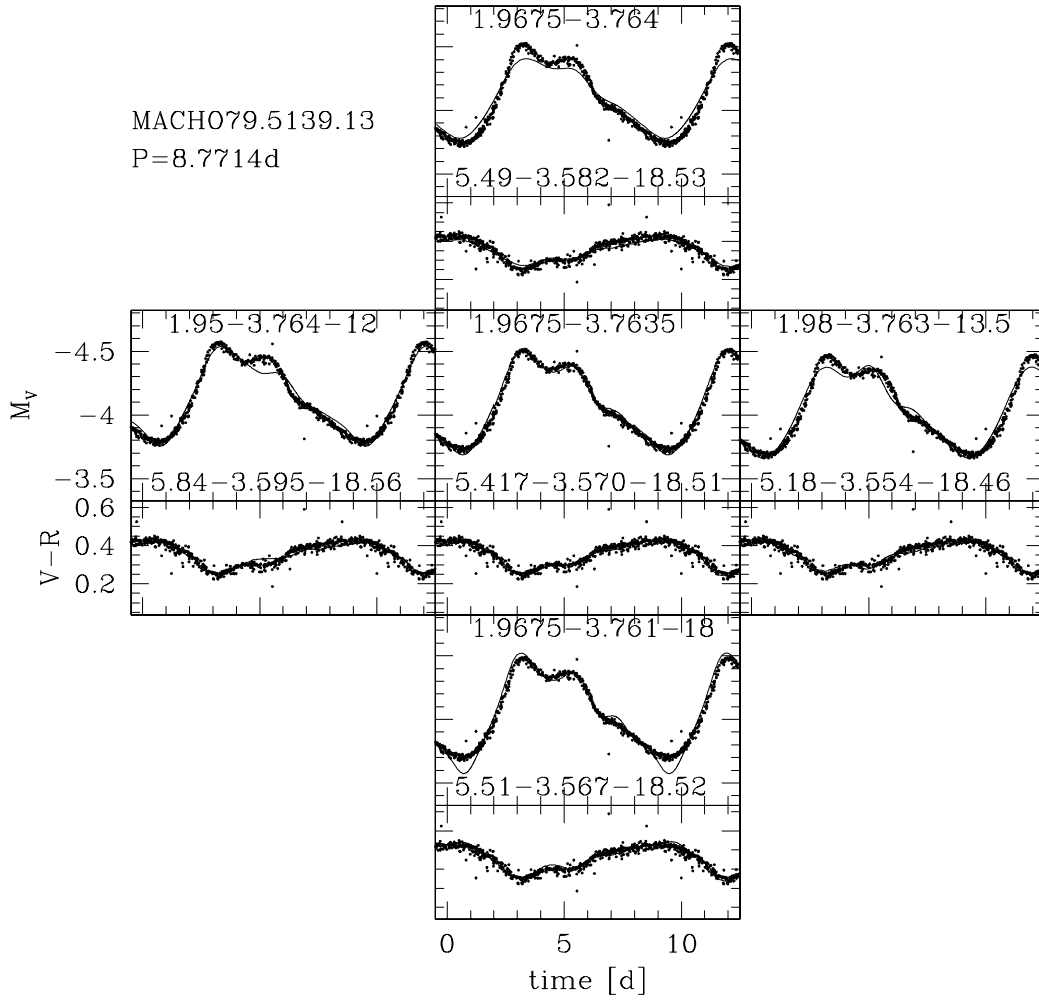


Fig. 3.— As in Fig. 2, model fits for MACHO 79.5139.13.

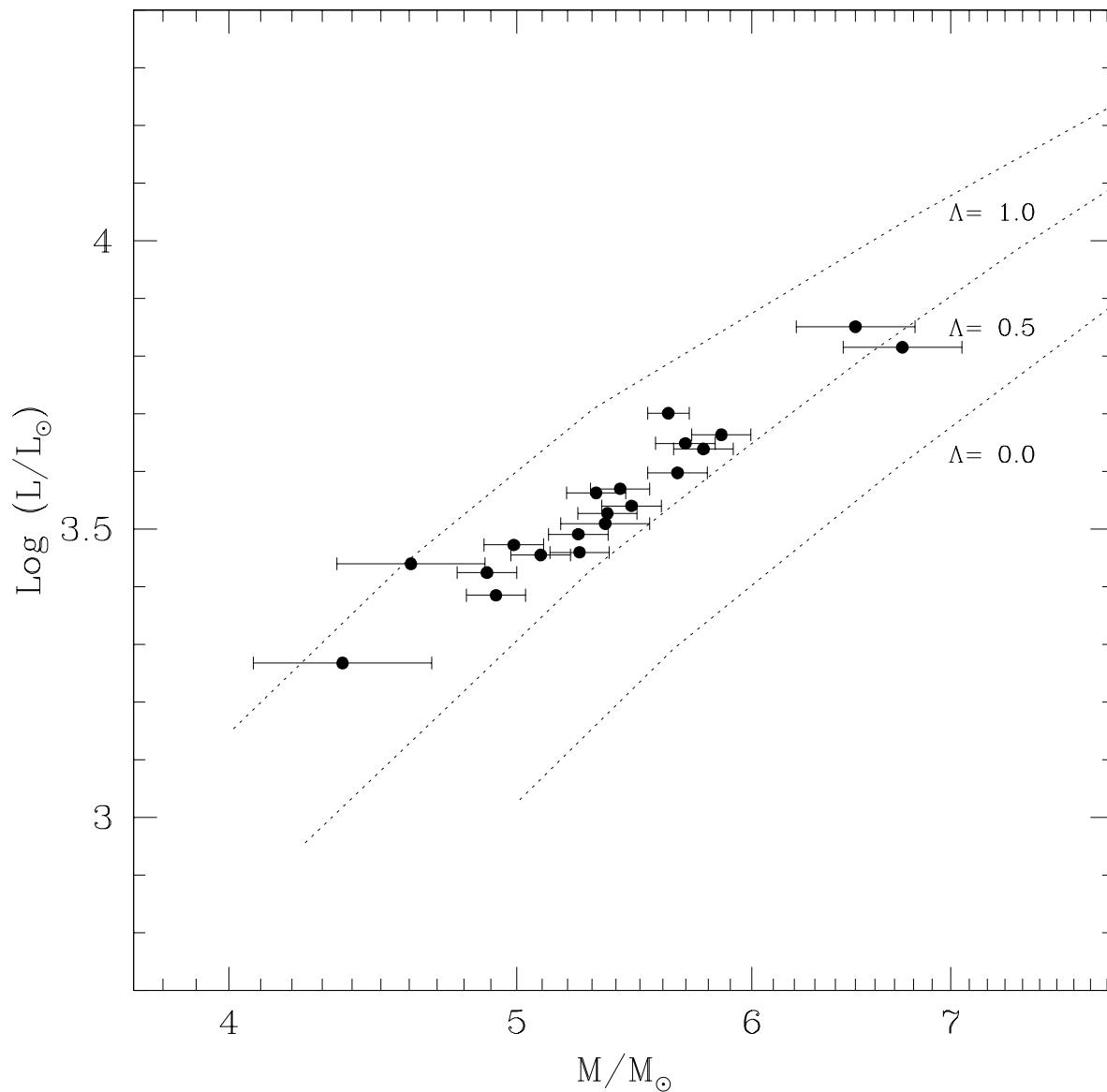


Fig. 4.— The mass-luminosity relation for the present sample of 20 bump Cepheids. Error bars are as discussed in the text. Overlaid are the M-L relations for core-He burning stars from Fagotto et al. (1994) and Bressan (2001) for three assumptions of the efficiency of convective core overshoot and $Z=0.008$ and $Y=0.25$. The solid line represent the best match to the data ($\Lambda_c=0.65 l/H_p$).

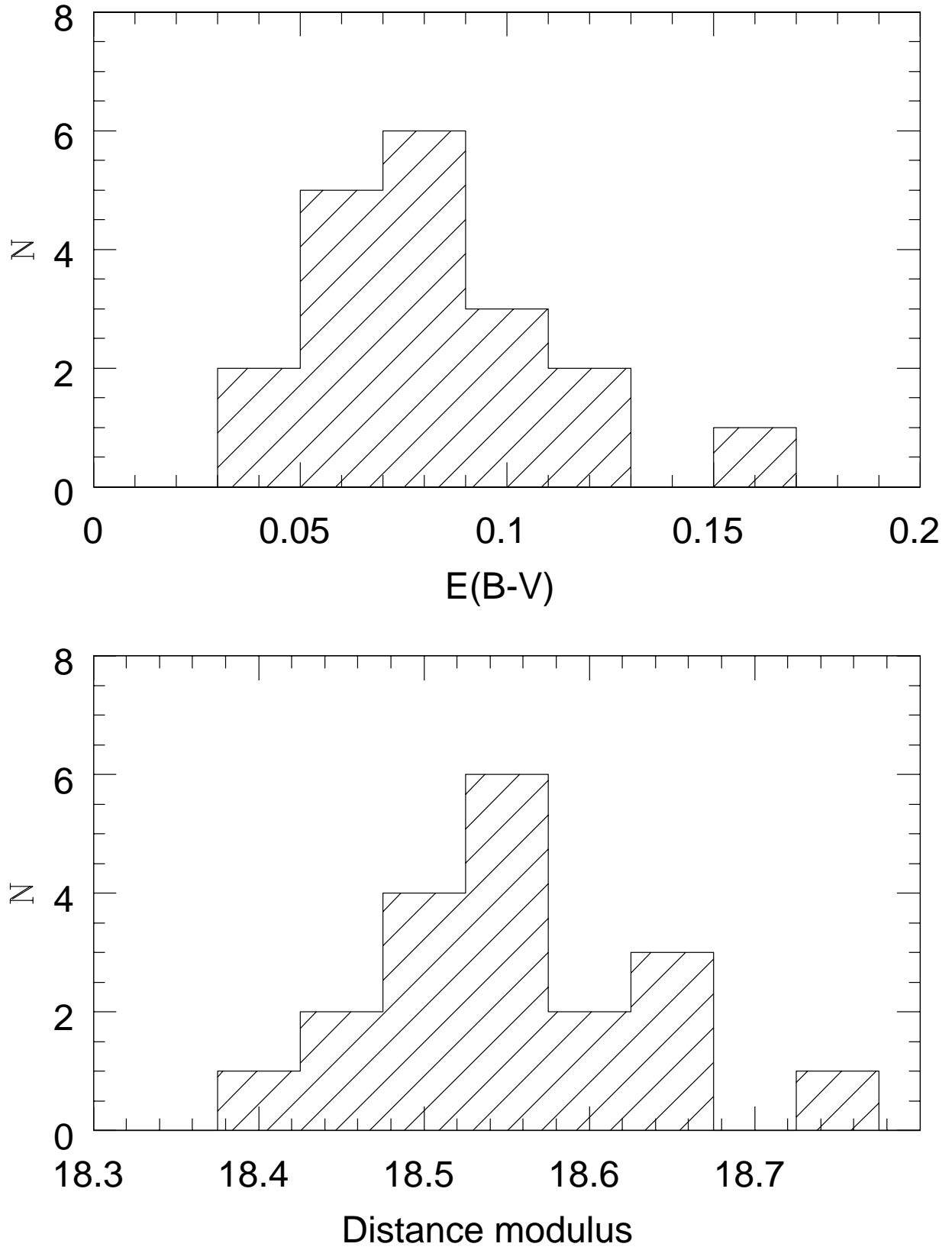


Fig. 5.— Histograms of the derived reddenings (top) and distance moduli (bottom) for the 20 Cepheids of our sample.

Table 1: The selected MACHO bump Cepheid sample

<i>MACHO</i> star id	RA (J2000)	Dec (J2000)	$\langle V \rangle$	$\langle V-R \rangle$	$P[d]$
1.3441.15	05 01 52.0	-69 23 22	14.45	0.37	10.4136
1.3692.17	05 02 51.4	-68 47 06	14.53	0.39	10.8552
1.3812.15	05 03 57.3	-68 50 25	14.61	0.39	9.7118
1.4048.6	05 05 08.8	-69 15 12	14.77	0.36	7.7070
1.4054.15	05 05 42.1	-68 51 06	14.93	0.37	7.3953
2.4661.3597	05 09 16.0	-68 44 30	14.32	0.39	11.85911
6.6456.4346	05 20 23.1	-70 02 33	15.16	0.36	6.4816
9.4636.3	05 09 04.5	-70 21 55	14.16	0.41	13.6315
9.5240.10	05 13 10.1	-70 26 47	15.11	0.38	7.3695
9.5608.11	05 15 04.7	-70 07 11	14.81	0.35	7.0693
18.2842.11	04 57 50.2	-68 59 23	14.83	0.38	8.8311
19.4303.317	05 06 39.8	-68 25 13	14.65	0.37	8.7133
19.4792.10	05 09 36.9	-68 02 44	14.96	0.36	6.8628
77.7670.919	05 27 55.1	-69 48 05	14.85	0.34	7.4423
77.7189.11	05 24 33.3	-69 36 41	14.73	0.39	7.7712
78.6581.13	05 20 56.0	-69 48 19	14.97	0.36	6.9302
79.4657.3939	05 08 49.4	-68 59 59	14.23	0.43	13.8793
79.4778.9	05 09 56.3	-68 59 41	14.56	0.33	8.1868
79.5139.13	05 11 53.1	-69 06 49	14.59	0.38	8.7716
79.5143.16	05 12 18.8	-68 52 46	14.61	0.34	8.2105

Table 2: The details of our sample

<i>MACHO</i> star id	P [d]	P_{02}	$\log(T_{eff})$	$E(B - V)$	μ_{obj}	$\log(L/L_{\odot})$	M/M_{\odot}
1.3441.15	10.4136	2.005	3.757	0.078	18.554	3.649	5.698
1.3692.17	10.8552	2.012	3.756	0.072	18.622	3.653	5.793
1.3812.15	9.7118	1.980	3.762	0.076	18.569	3.639	5.778
1.4048.6	7.7070	1.938	3.765	0.060	18.626	3.455	5.093
1.4054.15	7.3953	1.940	3.767	0.065	18.563	3.472	4.988
2.4661.3597	11.8591	2.030	3.755	0.088	18.548	3.701	5.623
6.6456.4346	6.4816	1.940	3.770	0.093	18.665	3.267	4.368
9.4636.3	13.6315	2.035	3.756	0.078	18.478	3.851	6.501
9.5240.10	7.3695	1.952	3.767	0.082	18.477	3.439	4.606
9.5608.11	7.0693	1.92	3.765	0.155	18.735	3.460	5.249
18.2842.11	8.8311	1.973	3.762	0.049	18.431	3.563	5.317
19.4792.10	6.8628	1.924	3.766	0.051	18.548	3.424	4.886
19.4303.317	8.7133	1.958	3.763	0.068	18.564	3.597	5.663
77.7670.919	7.4423	1.936	3.765	0.078	18.543	3.491	5.244
77.7189.11	7.7712	1.940	3.764	0.092	18.501	3.509	5.355
78.6581.13	6.9302	1.930	3.764	0.084	18.540	3.385	4.920
79.4657.3939	13.8793	2.032	3.758	0.112	18.528	3.815	6.742
79.4778.9	8.1868	1.953	3.762	0.071	18.643	3.527	5.364
79.5139.13	8.7716	1.968	3.763	0.068	18.509	3.570	5.417
79.5143.16	8.2105	1.95	3.763	0.114	18.571	3.540	5.465